Appendix

Inverse DMO

§ A.1 Prestack full migration

The presence of a single spike in the dataset, at travel time $t = t_h$, with shot at $(x, y, z) = (h, 0, 0)$ and receiver at $(-h, 0, 0)$, means that there is an ellipsoidal reflector at all points (x, y, z) such that the sum of the distance from a point (x, y, z) on the reflector to the source $\sqrt{(x-h)^2+y^2+z^2}$, plus the distance from that point to the receiver $\sqrt{(x+h)^2+y^2+z^2}$, equals the travel time times the velocity:

$$\sqrt{(x-h)^2+y^2+z^2} + \sqrt{(x+h)^2+y^2+z^2} = vt_h \ . \tag{A.1.1}$$

The ellipsoid in equation (A.1.1) can be written as

$$\left(\frac{x}{a_x}\right)^2 + \left(\frac{y}{a_y}\right)^2 + \left(\frac{z}{a_z}\right)^2 = 1 \ . \tag{A.1.2}$$

a_x can be found by setting $z = 0$ and $y = 0$ in equation (A.1.1):

$$a_x = vt_h/2 \ . \tag{A.1.3}$$

Similarly,

$$a_y = a_z = \sqrt{(vt_h/2)^2 - h^2} = vt_n/2 \ , \tag{A.1.4}$$

where t_n is the normal moveout (NMO) time:

$$t_n^2 = t_h^2 - (2h/v)^2 \ . \tag{A.1.5}$$

Prestack migration of an impulse therefore produces the ellipsoid

$$\left(\frac{x}{vt_h/2}\right)^2 + \left(\frac{y}{vt_n/2}\right)^2 + \left(\frac{z}{vt_n/2}\right)^2 = 1 \ . \tag{A.1.6}$$

Using equation (A.1.5) we have

$$\frac{x^2}{1+(2h/vt_n)^2} + y^2 + z^2 = \left(vt_n/2\right)^2 \ . \tag{A.1.7}$$

The change of variable

$$\chi^2 = \frac{x^2}{1 + (2h/vt_n)^2} \tag{A.1.8}$$

compresses the ellipsoid (A.1.7) to the sphere

$$\chi^2 + y^2 + z^2 = (vt_n/2)^2 , \tag{A.1.9}$$

which is the zero-offset migration of a spike at the NMO time t_n .

Zero-offset migration is described by the dispersion relation

$$\left(\frac{v}{2}\right)^2 \left(k_\chi^2 + k_y^2 + k_z^2\right) = \omega_n^2 . \tag{A.1.10}$$

Inserting the Fourier transform of the change of variables (A.1.8)

$$k_\chi^2 = k_x^2 \left[1 + (2h/vt_n)^2\right] , \tag{A.1.11}$$

into equation (A.1.10) gives

$$\left(\frac{v}{2}\right)^2 \left(k_x^2 + k_y^2 + k_z^2\right) = \omega_n^2 - \left(\frac{hk_x}{t_n}\right)^2 . \tag{A.1.12}$$

This is the dispersion relation for prestack, post-NMO, full migration.

§ A.2 Prestack partial migration

Prestack full migration (Figure A.2.1) can be done in three steps:

(1) NMO.

(2) Prestack partial migration (DMO): substitute

$$\omega_0^2 = \omega_n^2 - \left(\frac{hk_x}{t_n}\right)^2 \tag{A.2.1}$$

on the right-hand side of equation (A.1.12). Equation (A.2.1) is time dependent: ω_n and t_n appear together. It is velocity independent (but constant velocity was assumed).

(3) Migration: using the dispersion relation:

$$\left(\frac{v}{2}\right)^2 \left(k_x^2 + k_y^2 + k_z^2\right) = \omega_0^2 . \tag{A.2.2}$$

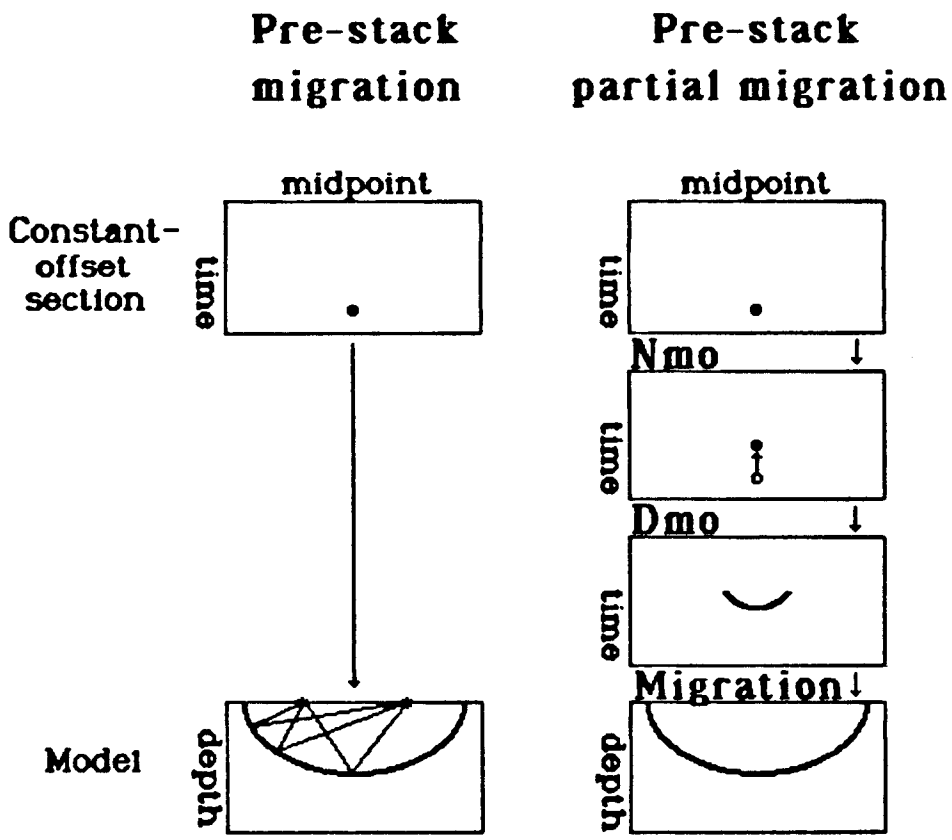

FIG. A.2.1. Decomposition of prestack full migration to NMO, DMO, and poststack migration.

§ A.3 Inverse DMO

The relation (A.2.1) can be used to derive the relation between the zero-offset section m and the common-offset section d.

Starting from the inverse Fourier transform

$$d\,(t_n\,,k_x\,,h\,) = \int d\,\omega_n\, e^{-i\,\omega_n\,t_n}\; d\,(\omega_n\,,k_x\,)\,, \tag{A.3.1}$$

and changing variables ω_n to ω_0, we have

$$= \int d\,\omega_0 \left|\frac{d\,\omega_n}{d\,\omega_0}\right| e^{-i\,\omega_n\,(\omega_0,t_n\,,h\,,k_x\,)t_n}\; d\,[\omega_n\,(\omega_0,t_n\,,h\,,k_x\,),k_x\,,h\,]$$

$$= \int d\,\omega_0 \left|\frac{d\,\omega_n}{d\,\omega_0}\right| e^{-i\,\omega_n\,(\omega_0,t_n\,,h\,,k_x\,)t_n}\; m\,(\omega_0,k_x\,)\,, \tag{A.3.2}$$

where $\omega_n\,(\omega_0,t_n\,,h\,,k_x\,)$ is given by equation (A.2.1). Defining

$$A = \sqrt{1 + (hk_x/\omega_0 t_n)^2}\ , \tag{A.3.3}$$

we have

$$\omega_n = A\,\omega_0\ , \tag{A.3.4}$$

and

$$\left| \frac{d\,\omega_n}{d\,\omega_0} \right| = \left| \frac{\omega_0}{\omega_n} \right| = A^{-1}\ . \tag{A.3.5}$$

Substituting equations (A.3.4) and (A.3.5) into (A.3.2), we finally get

$$d\,(t_n, k_x, h) = \int d\,\omega_0\, A^{-1}\, e^{-i\,\omega_0 A t_n}\, m\,(\omega_0, k_x)\ . \tag{A.3.6}$$

§ A.4 Impulse responses

Deregowski and Rocca (1981) showed that DMO will smear an impulse at $(x=0, t=t_n)$ to the ellipse

$$t_0^{\,2}\,(x) = t_n^{\,2}\left(1 - \frac{x^2}{h^2}\right)\ . \tag{A.4.1}$$

The inverse DMO will therefore smear an impulse at $(x=0, t=t_0)$ to the curve

$$t_n^{\,2}(x) = \frac{t_0^{\,2}}{\left(1 - \frac{x^2}{h^2}\right)}\ . \tag{A.4.2}$$

The DMO and inverse DMO impulse responses are shown in Figure A.4.1. Applications of inverse DMO after DMO ($\mathbf{D}^{+}\mathbf{D} \approx \mathbf{I}$), and DMO after inverse DMO ($\mathbf{D}\mathbf{D}^{+} \approx \mathbf{I}$), are shown in Figure A.4.2.

§ A.5 Inverse DMO in three dimensions

In equation (A.1.1), I made the assumption that the shot and receiver lie along the x axis. In general, however, they do not, and the half-offset is a vector

$$\mathbf{h} = \begin{pmatrix} h_x \\ h_y \end{pmatrix}\ . \tag{A.5.1}$$

Let θ be the angle of rotation such that

$$\mathbf{h} = \begin{pmatrix} \cos\theta \\ \sin\theta \end{pmatrix} h\ , \qquad h = \sqrt{h_x^{\,2} + h_y^{\,2}}\ . \tag{A.5.2}$$

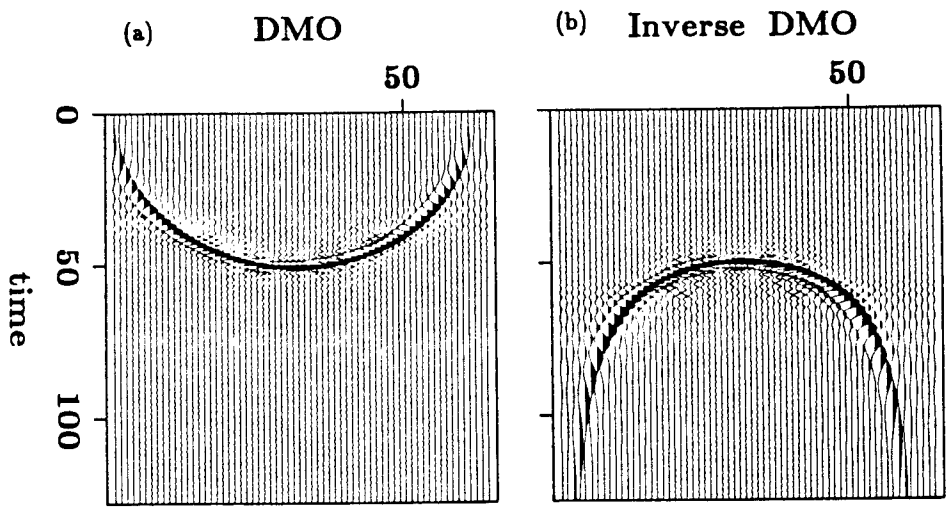

FIG. A.4.1. (a) DMO impulse response. (b) Inverse DMO impulse response.

We can rotate the $(x\,,y\,)$ axes to $(x'\,,y'\,)$ by

$$\begin{pmatrix} x' \\ y' \end{pmatrix} = \begin{pmatrix} \cos\theta & \sin\theta \\ -sin\ \theta & \cos\theta \end{pmatrix} \begin{pmatrix} x \\ y \end{pmatrix}, \tag{A.5.3}$$

so that the shot and receiver lie along the x' axis, as in equation (A.1.1), and we can make the same development of equations (A.1.1) through (A.3.6) in $(x'\,,y'\,)$ coordinates, obtaining

$$d\,(t_n\,,k_{x'}\,,k_{y'}\,,h\,) = \int d\,\omega_0\,A^{-1}\,e^{-i\,\omega_0 A t_n}\,m\,(\omega_0,k_{x'}\,,k_{y'}\,)\,, \tag{A.5.4}$$

with

$$A\ = \sqrt{1 + (hk_{x'}\,/\omega_0 t_n\,)^2}\,. \tag{A.5.5}$$

To return to the original coordinates, recall that rotation at the space domain corresponds to a rotation in the same direction at the frequency domain:

$$\begin{pmatrix} k_{x'} \\ k_{y'} \end{pmatrix} = \begin{pmatrix} \cos\theta & \sin\theta \\ -sin\ \theta & \cos\theta \end{pmatrix} \begin{pmatrix} k_x \\ k_y \end{pmatrix}. \tag{A.5.6}$$

So,

$$\begin{aligned} hk_{x'} &= h\,(\cos\theta\ k_x\ + \sin\theta\ k_y\,) \\ &= (h\,\cos\theta)k_x\ + (h\,\sin\theta)k_y \\ &= h_x\,k_x\ + h_y\,k_y \end{aligned} \tag{A.5.7}$$

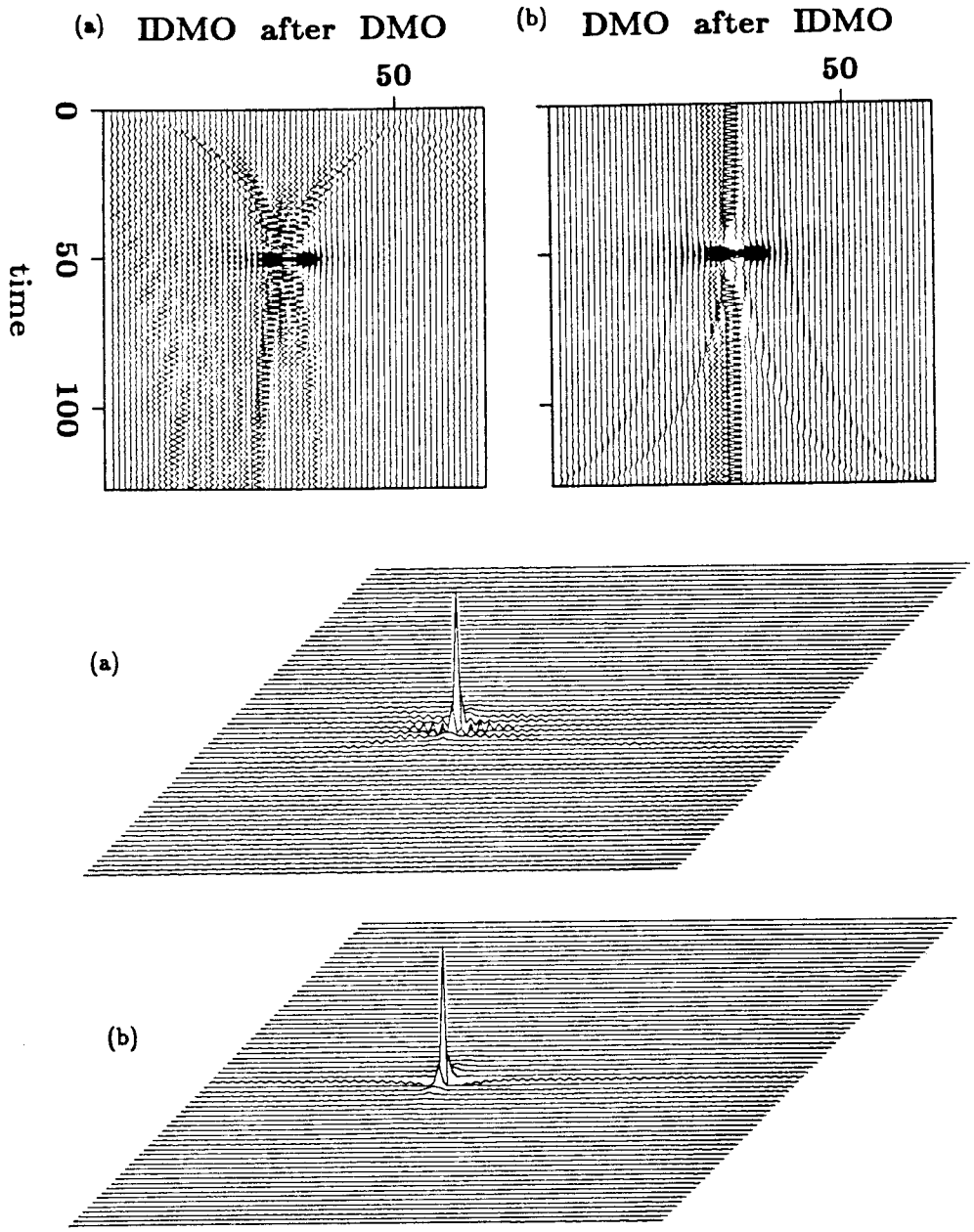

FIG. A.4.2. (a) Inverse DMO after DMO of an impulse. (b) DMO after inverse DMO of an impulse.

$$= \mathbf{h}\cdot\mathbf{k} \ ,$$

and equations (A.5.4) and (A.5.5) become

$$d\,(t_n\,,k_x\,,k_y\,,h\,) = \int d\,\omega_0\,A^{-1}\,e^{-i\,\omega_0 A t_n}\,m\,(\omega_0,k_x\,,k_y\,)\ , \tag{A.5.8}$$

where

$$A = \sqrt{1+(\mathbf{h}\cdot\mathbf{k}/\omega_0 t_n)^2} \,. \tag{A.5.9}$$

§ A.6 Summary

DMO and its pseudo-inverse are given by Table A.6.1.

DMO	$m(\omega) = \int dt \; A^{-1} \, e^{-i\omega A t} \, d(t,h)$
Inverse DMO	$d(t,h) = \int d\omega \, A^{-1} \, e^{i\omega A t} \, m(\omega)$

TABLE A.6.1. The DMO is a unitary-like operator since its pseudo-inverse is also its complex conjugate.

קשת י"ג בכסלו תשמ"ו

KESHET Nov. 30, 1985